Volume 15, Issue 2, 152517 (1-15)

Iranian Journal of Catalysis (IJC)

https://doi.org/10.57647/j.ijc.2025.1502.17

One-pot synthesis of 2-amino-4H-chromene derivatives catalysed by Fe_3O_4@SiO_2@Mg-Al-LDH as an efficient and reusable magnetic nano- catalysts

Raju Shekhanavar[1], Santosh Khatavi[1], Balachandra G. Hegde[2], Kamanna Kantharaju[1,*]

[1]*Department of Chemistry, Rani Channamma University, Belagavi, Karnataka, India.*
[2]*Department of Physics, Rani Channamma University, Belagavi, Karnataka, India.*

[*]**Corresponding author:** kk@rcub.ac.in

Original Research

Received:
9 August 2024
Revised:
28 October 2024
Accepted:
12 February 2025
Published online:
17 March 2025

Abstract:

This work describes the environmentally friendly preparation of Fe_3O_4 utilizing agro-waste orange peel ash aqueous extract as a solvent medium, and then it functionalized to SiO_2@Mg-Al-LDH under ultrasonication. Further, these prepared materials were characterized by FT-IR, XRD, FE-SEM, EDX, and VSM. Furthermore, it demonstrated the application of this functionalized iron oxide for the synthesis of 2-amino-4H-chromene derivatives. The synthesis routed via a one-pot three-component reaction (3CRs) of aryl/heterocyclic aldehyde, malononitrile, and resorcinol under MWI at 180W using EtOH as a solvent gave excellent product isolation achieved in a short reaction time. The catalyst is very efficient towards both electron-withdrawing and electron-donating groups present on aryl or heterocyclic aldehydes. The magnetic nature of this catalyst allows it to be easily separated by a permanent magnetic field, and catalysts can be reused several times without losing significant catalytic activity. Additionally, selected synthesized chromene derivatives were tested for their antimicrobial properties using agar media. The compounds **4b**, **4c**, and **4d** showed comparable activity tested against bacteria and fungi.

Keywords: Agro-waste; Excellent yield; Magnetic nanoparticles; 2-amino-4H-chromene; Microwave irradiation

1. Introduction

Numerous applications of heterocyclic compounds have been explored in pharmaceuticals, chemical industries, agrochemicals, and pesticides, and they emerged as valuable molecules [1]. Heterocyclic compounds are widely used in various research areas due to their ability to construct complex structural skeletons to achieve desired functions [2]. Hence, large numbers of organic chemists are interested in the construction of heterocyclic molecules, especially oxygen-containing heterocycles [3] such as 4H-pyrans and 4H-pyran-annulated heterocyclic scaffolds [4], due to their ubiquitous presence in the nature, and they also provide appropriate biological activities [5]. Presence of certain substituents present in the molecules [6], and these functional derivatives can develop anti-HIV [7], anti-tumor [8], antimicrobial [9], anti-inflammatory [10], antifungal [11], and anti-allergenic properties [12]. In addition, pyran-containing heterocyclic compounds are prevalent in nature and are increasingly used in pharmaceuticals [13], biodegradable agrochemicals [14], pigments [15], and cosmetics [16]. In most cases [17], these compounds are isolated and purified through a difficult process that uses limited natural resources [18]. It has, therefore, been a priority to investigate the progress of the derivatives and their potential therapeutic properties in order to synthesize compounds [19]. Several synthetic procedures have been developed for the one-pot Knoevenagel condensation of C–H activated acids [20], aldehydes, and malononitrile to prepare functionalized 2-amino-4H-chromene derivatives using various catalyst such as SDS [21], DAHP [22], MNP@AVOPc [23], [Sipim]HSO_4 [24], nano-Al_2O_3 [25], POPINO [26–30], CuO NPs [31] and TBBDA [32]. However, several limitations/drawbacks are associated with these methods, such as lower yields, prolonged reaction time, toxicity, poor catalyst

recovery, and tedious work-up [33]. Due to this, there still exists a high demand for modest, versatile, and environmentally friendly processes to synthesize 2-amino-4H-chromene derivatives [34]. As part of green chemistry trends, scientists strive to prevent the use of hazardous substances or generate chemical waste and are concerned with developing novel and efficient greener methodologies [35]. In most cases, solvent-free conditions in chemical processes play a crucial role in solving these problems, even if innovative processes with environmentally friendly solvents are used [36]. In recent years, various simple synthetic routes were developed; among these, magnetic nanoparticles (MNPs) served as catalysts that provide solvent-free separation procedures, thereby eliminating most of the tedious separation procedures associated with the use of organic solvents [37]. In the industrial sector, metal-catalysis is playing a significant role [38]. It is definitive that transition-metal nanoparticles can be used for catalysis due to their ability to activate metal surfaces at the nanoscale, thereby enhancing heterogeneous catalysis efficiency and selectivity [39]. In the preparation of MNPs and their modifications achieved, since they are stable, low toxic, easy to synthesize and functionalize, and have large surface area, they are an effective catalytic material. The anisotropic dipolar attraction of Fe_3O_4 nanoparticles leads to loss of dispersibility and catalytic activities. Therefore, this type of uncoated nanoparticles can easily aggregate into large clusters, and their magnetic properties are also lost due to the acidic environment [40]. But, when exposed to biological systems, Fe_3O_4 nanoparticles are likely to undergo rapid biodegradation, even if they are relatively small [41]. To overcome some of these limitations, it is essential to functionalize the core with a protective layer of silica or any other coating materials that are well-reported [42]. In order to prepare heterogeneous catalysis, it is of paramount importance to present magnetic-coated nanoparticles as a suitable alternative support [43]. In this study, we have synthesized 2-amino-4H-chromene derivatives catalyzed by Fe_3O_4@SiO_2@Al-Mg-LDH. The required catalyst core was prepared using eco-friendly and non-toxic novel. The coated SiO_2-LDH on MNPs was found to be efficient and easily recyclable using an external magnet.

2. Experimental

For this work, the reagent was used as it was received directly from vendors (AVRA). An XRD sample was collected through X-pert PRO, an analytical spectrum was collected through Lambda-750, and an SEM-EDX sample was collected by EVOLS15 Germany Model Zeiss. With a Perkin Elmer FT-IR, the KBr pellet method.

2.1 Preparation of orange peel water extract

The required orange peels were collected from the local juice center. To remove any physical impurities on the surface washed with tap water, and then dried in sunlight. A Bunsen burner is used to convert the orange peel into ash. Obtained 10 grams of ash added in 100 mL of double distilled water in a beaker and stirred for one hour at room temperature. After stirring, the filtered mixture was removed from the suspension, which resulted in a light brown filtrate named Water Extract of Orange Fruit Peel Ash (WEOFPA), which was used for the preparation of MNPs.

2.2 Preparation of Fe_3O_4 using WEOFPA

In a 100 mL beaker, 50 mL of double distilled water and 10 mL of WEOFPA were mixed with 3.2 g of $FeSO_4$. $7H_2O$ and 3.4g of $FeCl_3.6H_2O$. A black precipitate was formed after heating the mixture to 85 °C for 45 min, then cooling it to room temperature, and adding NaOH dropwise until a black precipitate formation cease. A strong magnet was used to collect the precipitate after the 1-hour precipitation settlement. It was washed several times with double distilled water, followed by ethanol. A muffle furnace with a temperature of 700 °C was used to dry and calcin the residue, and then materials were kept in the desiccator for further use (Fig. 1).

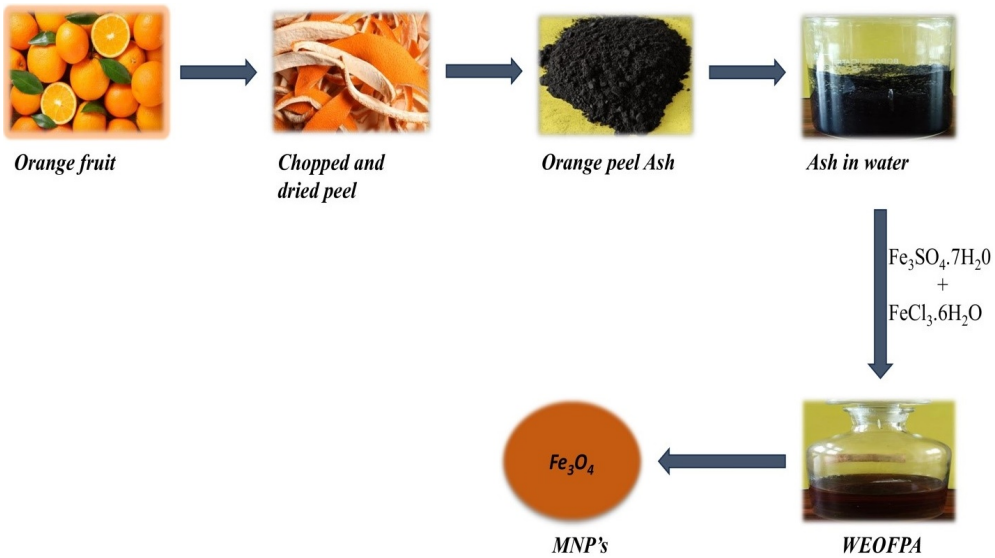

Figure 1. Preparation of Fe_3O_4 using WEOFPA.

2.3 Preparation of MNPs coated silica (Fe_3O_4@SiO_2)

A method for preparing Fe_3O_4@SiO_2 nanoparticles has been described previously [44]. Briefly, the prepared 1.5 g Fe_3O_4 above procedure was dispersed in ethanol (6 mL) and water (4 mL) under ultrasonication, and then slowly added NaOH solution (4 mL, 25 weight%), continued ultrasonication till black precipitate formation stopped. In the next step, the reaction mixture was stirred under magnetic stirring. To this, we slowly added tetraethyl orthosilicate (TEOS) in ethanol (1 mL/10 mL) dropwise and dispersed. After the reaction, cooled to rt, using an external magnet, held coated materials, and washed with distilled water one time, followed by two times ethanol solvent. The obtained precipitate dried @ 60 °C under a vacuum oven for 8 h and stored in an airtight container in a desiccator.

2.4 Preparation of Fe_3O_4@SiO_2@Mg-Al LDH

Taken 1.6 g NaOH and 1.28 g Na_2CO_3 in 100 mL of 1:1 (v:v) methanol-water solution to prepare a pH buffered solution for pH adjustment of 1.5 g Fe_3O_4@SiO_2 microsphere particles. To this 20 mL mixture containing 1.44 mmol of Mg $(NO_3)_2$. $6H_2O$ and 0.48 mmol of Al $(NO_3)_3$. $9H_2O$ were added at a rate of 1 mL/min drop-wise, and the pH of the solution was maintained at 10, and the suspension was stirred vigorously and then transferred to ultrasonication for product dispersion about 1 h, and then collected product further ultrasound dispersed for an additional 1 h in deionized water. Finally, an external magnet was used to collect the product (Fe_3O_4@SiO_2@Mg-Al LDH) from the solution, washed with water and ethanol, then dried at 60 °C under a vacuum oven (Fig. 2).

2.5 Spectral data of some selected derivatives

2-Amino-4-(4-(dimethylamino) phenyl)-7-hydroxy-4H-chromene-3-carbonitrile ***(4a)***

Yellow; FT-IR (cm^{-1}, KBr): 3490 (OH), 3292 (NH_2), 3063 (CH), 2212.06 (CN), 1719 (C=O); ^{1}H NMR (400 MHz, DMSO-d_6): (δ ppm) 2.45 (CH_3, s, 3H), 2.45 (CH_3, s, 3H), 4.46 (CH, s, 1H), 6.00 (CH, d, 1H), 6.10 (CH, s, 1H), 6.48-6.80 (Ar-H, m, 4H, J = 6.4), 7.78 (NH, s, 1H), 8.02 (OH, s, 1H); ^{13}C-NMR (100 MHz, DMSO-d_6): δ 22.99, 39.88, 40.50, 42.56, 127.70, 128.73, 140.02, 169.77; LC-MS: m/z (Cal. $C_{18}H_{17}N_3O_2$) = 307.1374 $[M]^+$; m/z (Obs.) = 308.2482 $(M+H)^+$.

2-Amino-4-(5-bromo-2-hydroxyphenyl)-7-hydroxy-4H-chromene-3-carbonitrile ***(4b)***

Solid; Light yellow; FT-IR: 3336, (NH_2), 2973 (OH), 2886 (CN), 1380 (C=C), 1086; ^{1}H-NMR (400 MHz, DMSO-d_6) δ 6.95-6.98 (m, 1H), 7.45-7.47(m, 2H), 7.61-7.70 (m, 2H), 7.90-8.03 (m, 3H), 8.82 (s, 2H), 10.19 (s, 1H) ; ^{13}C-NMR (100 MHz, DMSO-d_6): δ 39.23, 40.28, 40.49, 103.86, 103.861, 111.16, 114.74, 115.978, 117.37, 119.50, 119.656, 120.342, 142.42, 131.78, 132.16, 137.97, 152.48, 153.55, 156.86, 160.29, 190.27; MS: m/z (Cal.$C_{16}H_{12}N_2O_2$) = 358.00 $[M]^+$; m/z (Obs.) = 359.17$(M+H)^+$.

2-Amino-7-hydroxy-4-(pyridine-2-yl)-4H-chromene-3-carbonitrile ***(4c)***

Solid; Yellow; FT-IR (cm^{-1}): 3148 (NH_2), 2825 (CH), 2213 (CN), 1627, 1547 (C=O); ^{1}H-NMR (400 MHz, DMSO-d_6) δ 6.17-6.19 (m, 1H), 6.89-7.21(m, 2H), 7.50-7.59 (m, 2H), 7.99-8.84 (m, 5H), 9.21 (s, 1H) ; ^{13}C-NMR (100 MHz, DMSO-d_6): δ102.95, 106.69, 115.44, 121.83, 123.62, 128.91, 130.18, 137.61, 138.18, 150.71, 154.80, 158.86; LC-MS: m/z (Cal. $C_{18}H_{16}N_2O_4$) = 265.09 $[M]^+$; m/z (Obs.) = 267.00 $(M+H)^+$

2-Amino-4-(2-chloroquinolin-3-yl)-7-hydroxy-4H-chromene-3-carbonitrile ***(4d)***

Solid; Light Yellow; FT-IR (cm^{-1}): ν 3065 (NH_2), 2228 (C=N), 1564 (C=C), 1486, (C-Cl), cm^{-1}; ^{1}H-NMR (400 MHz, DMSO-d_6): 3.47 (s, H, CH), 7.75-7.79 (m, 2H, Ar), 7.96-8.03 (m, 4H), 8.16-8.18 (d, 1H, Ar), 7.26-7.45 (d, J = 8.8 Hz, 2H, Ar), 8.94-8.95 (s, 1H, OH), 9.02 (s, NH_2), 10.36 (s, OH); ^{13}C-NMR (100 MHz, DMSO-d_6): δ 128.32, 128.72, 129.10, 130.62, 134.24, 134.35, 140.76, 141.86, 148.26, 148.99, 149.41, 157.53, and 189.84 ppm; HR-MS (ESI): m/z (Cal.): 349.06, m/z (Obs.): 349.30 Da $(M+H)^+$.

3. Result and discussion

3.1 Preparation and characterization of the catalyst

Reported procedure adopted for the preparation of the iron oxide (Zhao et al.) [45]. Briefly, $FeCl_3.6H_2O$ and $FeSO_4.7H_2O$ in the presence of basic agro-waste WEOFPA as a new eco-friendly protocol employed for Fe_3O_4 NPs synthesis. This free-flowing MNPs powder was obtained using an inexpensive and chemical-free method. Further, the surface MNPs were functionalized by TEOS to increase their catalytic activity and stability (Fe_3O_4@SiO_2). Finally, obtained nanoflakes of Mg–Al-LDH were deposited onto Fe_3O_4@SiO_2 microspheres via ultrasonication (Fig. 2).

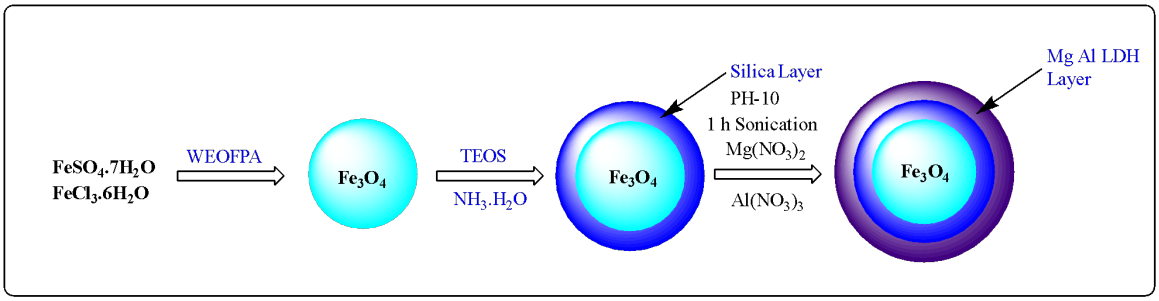

Figure 2. Pictorial representation of Fe_3O_4@SiO_2@Mg-Al-LDH preparation.

In addition to spectroscopic analysis, other microscopic methods were used to characterize materials, including scanning electron microscopes (SEM), X-ray diffraction (XRD), Fourier-transform infrared spectra (FT-IR), and vibrating sample magnetometers (VSM). The comparative IR spectra collected for the Fe_3O_4, Fe_3O_4@SiO_2, and Fe_3O_4@SiO_2@Mg-Al LDH were recorded between 400 to 4000 cm^{-1} (Fig. 3). The FT-IR band at 599 cm^{-1} represents Fe-O stretching of magnetic nanoparticles for all the materials. The IR band at 599 cm^{-1} represents the Fe-O stretching of all the materials. Two bands around 3401 cm^{-1} and 1633 cm^{-1} were observed due to O-H and C-O Stretching. In addition, the Si-O-Si asymmetric stretching vibration produces a wide and intense signal at 1096 cm^{-1}. At 802 cm^{-1}, symmetric stretching vibrations were observed for Si-OH bonds. Mg-O and Al-O vibrations are strongly correlated with the strong band at the lower wavenumber at 484 cm^{-1}. An XRD analysis was performed on free-flowing Fe_3O_4 powder, and diffraction showed clear 2θ peaks at 22.05°, 31.29°, 36.80°, 54.57°, 58.47°, and 63.84°; these data obtained are very much matching with JCPDS card no. 85-1436 [46–48]. Fe_3O_4@SiO_2 showed a peak at 13.87°, signifying silica on the surface of the shell, as well as a peak at 23.72°, 32.26°, 37.84°, 44.16°, 54.74°, 58.28°, and 63.83° indicating MNPs within the core. Additionally, the surface functionalization with Al-Mg-LDH the crystallinity of the material was lost, and peak at 26.5°, 39.75°, 43.0° and 76.52° are due to the Al, and peaks at 33.46°, 47.11° are due to the Mg present (figure S24), 16.68° and 18.62° attributable to silica, and peaks at 28.69°, 46.76°, 48.66°, and 63.84° attributable to Fe_3O_4 (Fig. 4).

SEM was used to investigate particle size and surface morphology of the Fe_3O_4, Fe_3O_4@SiO_2, and Fe_3O_4@SiO_2@Al-Mg-LDH. Using elemental mapping, the existence of Fe and O in Fe_3O_4 was confirmed (Fig. 5 (a) and 5 (d)). The surface morphology was altered when silica was applied on to the iron oxide surface, resulting in outer shell grooves (Fig. 5 (b)). In Fig. 5 (e) demonstrates elemental mapping, which clearly states the presence of Fe, Si, and O elements present in it. The FE-SEM images

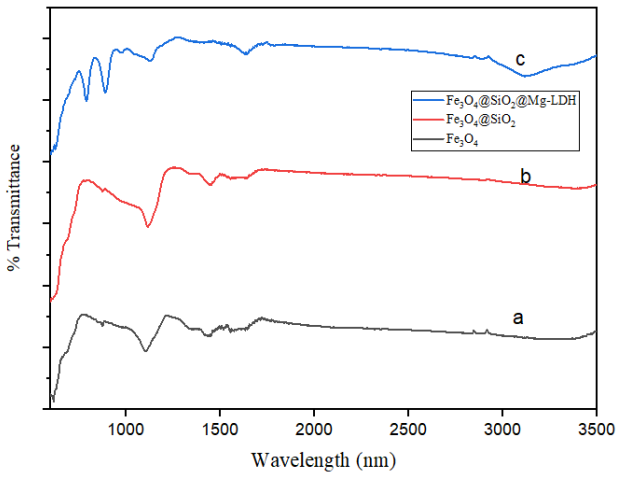

Figure 3. Comparative IR spectra of: (a) Fe_3O_4, (b) Fe_3O_4@SiO_2, and (c) Fe_3O_4@SiO_2@Mg-Al LDH.

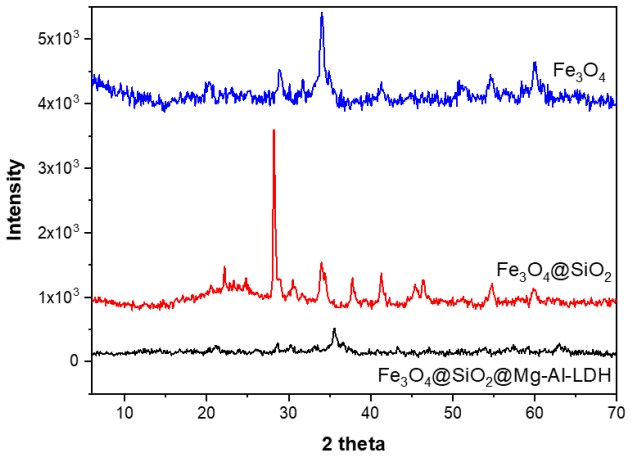

Figure 4. Comparative XRD spectra of: (a) Fe_3O_4, (b) Fe_3O_4@SiO_2 and (c) Fe_3O_4@SiO_2@Mg-Al LDH.

showed slight crystalline and porous shell structure after surface functionalization with Mg-Al-LDH. It was possible to determine the composition of Fe_3O_4@SiO_2@Mg-Al-LDH by elemental mapping (Figs. 5 (c) and 5 (f), and Fig. 6). We further validated the presence of elements in each modified MNPs by plotting counts versus energy in keV using Energy Dispersive X-ray Spectroscopy (EDS). Fe and O peak at 0.9, 6.18, 0.7, and 6.5 in the EDS plot of Fe_3O_4 confirmed composition. In Fig. 7, the EDS plot for Fe_3O_4@SiO_2 demonstrated the presence of a Si, confirmed the surface modification. Further, the EDS plot also revealed the presence of a peak at 1.2 Kev and 1.5 keV due to Mg and Al presence, respectively. Hence, the formation of Fe_3O_4@SiO_2@Mg-Al-LDH confirms the presence of Mg-Al-LDH in the modified MNPs, including other comparative peaks. A successful surface modification of MNPs was demonstrated in this study. The EDS spectra exhibited a Fe peak, with the Au peak consistently found as well due to the gold-sputtering. After MNPs were prepared using WE-OFPA, the spectral peaks at 0.1 and 3.9 reflect the presence of C and Ca, respectively. The EDS spectrum shows characteristic peaks corresponding to Si-33.84, Fe-2.56 wt%, and the presence of less quantity of elements Mg and Al, also confirmed the presence of these by qualitative analysis (Fig. 8).

3.2 Qualitative analysis of Mg and Al

Further to confirm presence of micro quantity of Al and Mg in LDH examined by qualitative analysis. Briefly, taken HCl: HNO_3 (1:3 mL) solution to dissolve Fe_3O_4@SiO_2@Mg-Al-LDH, and noticed clear solution (CS), the details of test is outlined in Table 1.

An applied field of 15 KG to −15 KG at room temperature used in a Vibrating Sample Magnetometer (VSM) to examine magnetic behaviour of Fe_3O_4, Fe_3O_4@SiO_2 and Fe_3O_4@SiO_2@Mg-Al LDH samples, as shown in the Fig. 9. From the M-H plot, can estimate the residual magnetization **(Mr)** and coercively **(Hc)** to expose the ferromagnetic nature (Table 2). Table 2 clearly shows the Mr values for Fe_3O_4 higher, and LDH values are considerably reduced after the substitution of SiO_2 and Mg-Al up to 12.65 emu/g.

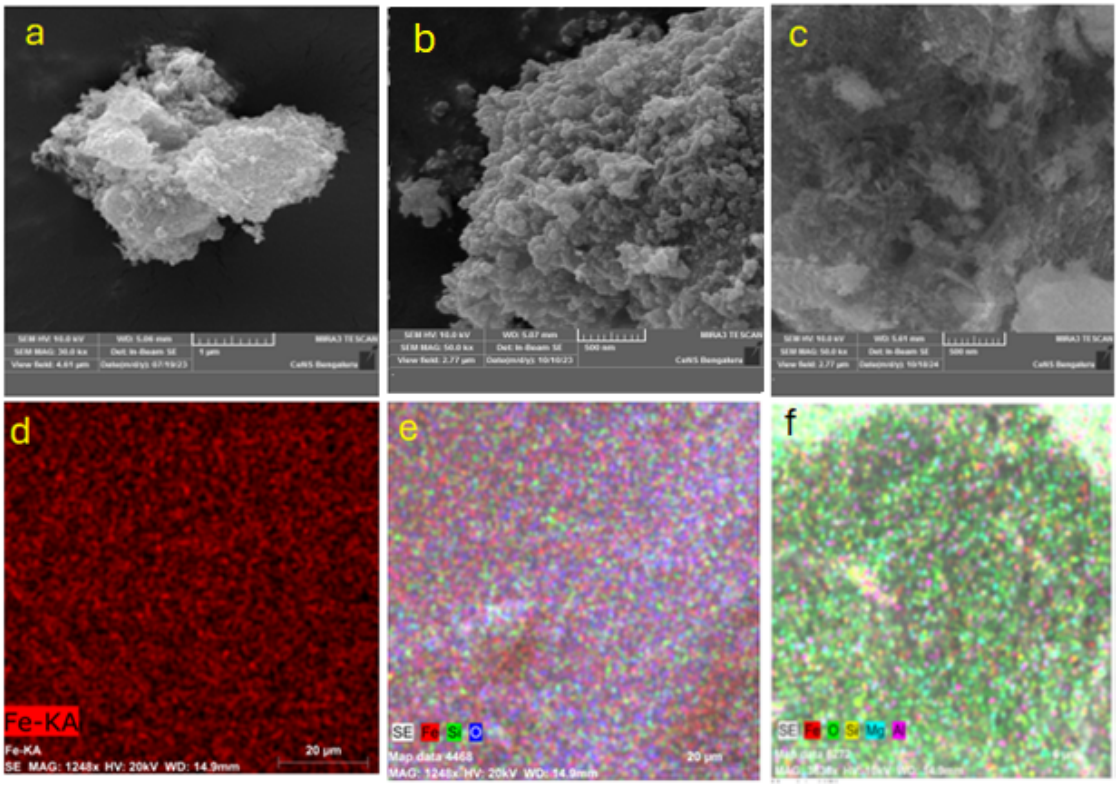

Figure 5. FE-SEM and elemental mapping of: Fe_3O_4 (a & d), Fe_3O_4@SiO_2 (b & e), and Fe_3O_4@SiO_2@LDH (c & f).

Based on this, it can be concluded that, for upper dopants there is reduction in magnetic saturation with increase in coercive force from 347.03 **(Oe)** to 360.53 **(Oe)** indicating gradual increase in the hardness as a substituent increases. It appears that, it is acting as a catalyst in the reaction based on the variation of magnetic behaviour. VSMs at RT and $-1\mathbf{T}$ to $+1\mathbf{T}$ fields were used to assess magnetic properties of the sample. Based on the magnetic properties: magnetic saturation/remainder magnetization, coercivity/hypersensitivity, and magnetic susceptibility/absorption, the results of

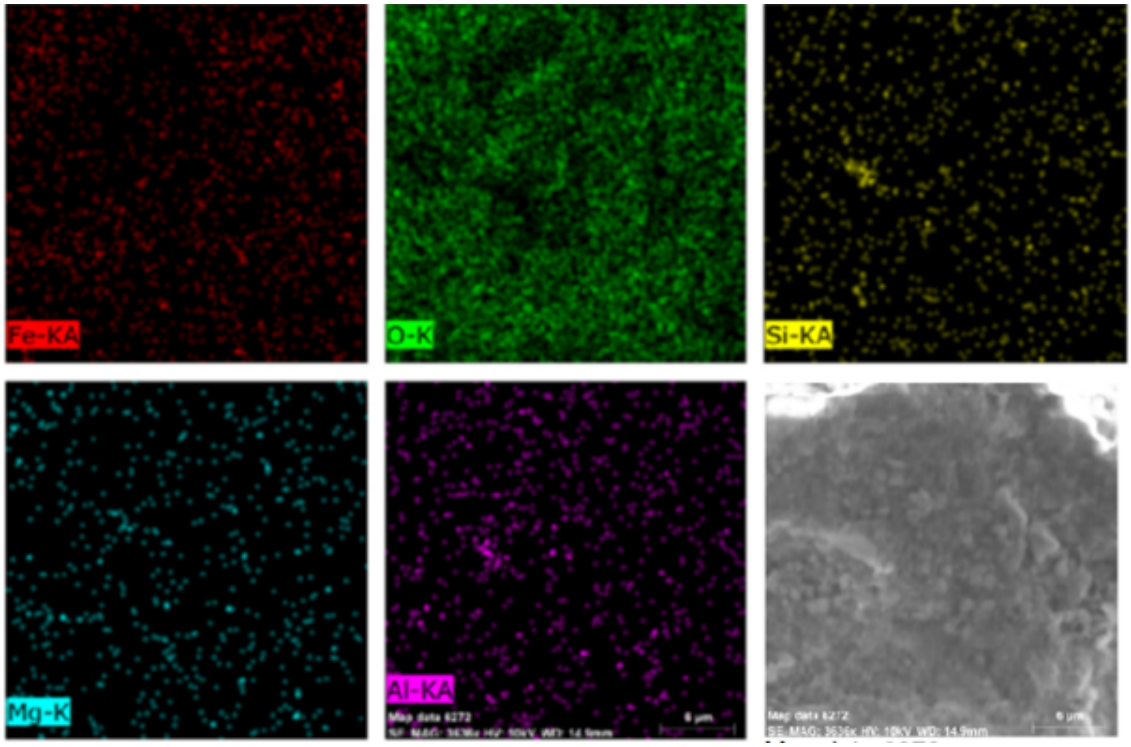

Figure 6. Elemental mapping of surface modified catalyst Fe_3O_4@SiO_2@LDH.

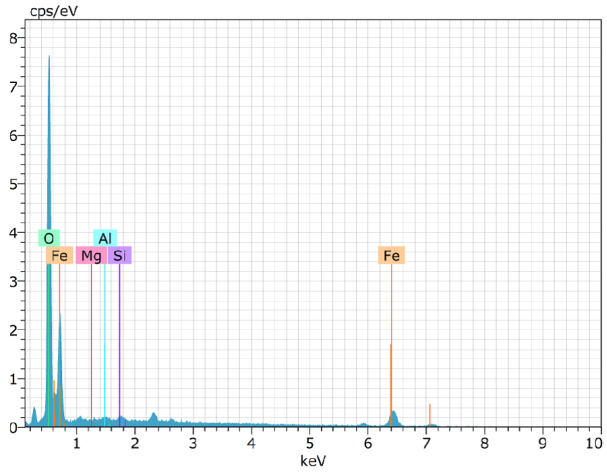

Figure 7. EDS analysis of Fe_3O_4@SiO_2@Mg-Al-LDH.

these properties are summarized in Table 2. In this case, Mr shows a significant difference from 36.11 emu/g to 12.65 emu/g since SiO_2 and Mg-Al LDH are neither magnetic nor antimagnetic in nature. However eventually, it exhibits magnetic saturation as Fe^{+3} ions replace SiO_2 and Mg-Al LDH creating free Fe^{+2}. In Table 2, Mr and Hc values measure the same level of support. According to Table 2, it also confirmed their magnetic susceptibilities are reduced when both SiO_2 and Mg-Al LDH are blended.

To explore the application of the prepared heterogeneous catalysts (Fe_3O_4@SiO_2@Al-Mg-LDH), herein demonstrated the catalytic activity towards Multicomponent Reactions (MCRs) of benzaldehyde (1), malononitrile (2), and resorcinol (3) as a model reaction for the synthesis of chromene derivatives at room temperature in ethanol solvent. The product isolated in solid, and completion of the reaction was monitored by TLC. The obtained crude product was dissolved in ethanol, and separated catalyst by external magnet gave low yield product isolation. This trail reaction taught us to use thermal energy to speed up the reaction as well improves product formation. Hence, in our laboratory extensively employed microwave-irradiation (MWI) technique to speed up the reaction rate in a model reaction resulted high yield isolation (Scheme 1).

A model reaction was used to optimize the reaction conditions. As a starting point 0, 5, 10, 20, 25, 30 and 35 mg of increasing catalyst loading taken in a series of model reaction under 300 W MWI power in ethanol solvent (5 mL). The isolated product yield with increasing catalysts loading from 5 to 25 mg noticed gradual increase of the isolated yield (entries 1-4, Table 3). Despite this, no change in the product isolation observed, when 30 and 35 mg of the catalyst loaded reaction (entries 5 & 6, Table 3). This optimization studies revealed that, 25 mg of catalysts is required to create one mmol of reaction with high yield in five minutes of irradiation gave (entry 4, Table 3). Surprisingly, no product formation noticed without catalysts under MWI, this confirms reaction required catalytic medium for the product formation (entry 1, Table 3).

To optimize required microwave power for the reaction screened using optimized catalysts amount (25 mg) in a model reaction in ethanol (5 mL). The series of variation of the MW power performed in a model reaction starting with 100 W to 600 W available in MW oven. This optimization experimental data is outlined in the Table 4. After MW power optimization, it was discovered reaction conducted at 300 W in five minutes achieved high product isolation. In light of this reaction, it was determined that MW power of 300 W and reaction duration of 5 min ideal for this reaction

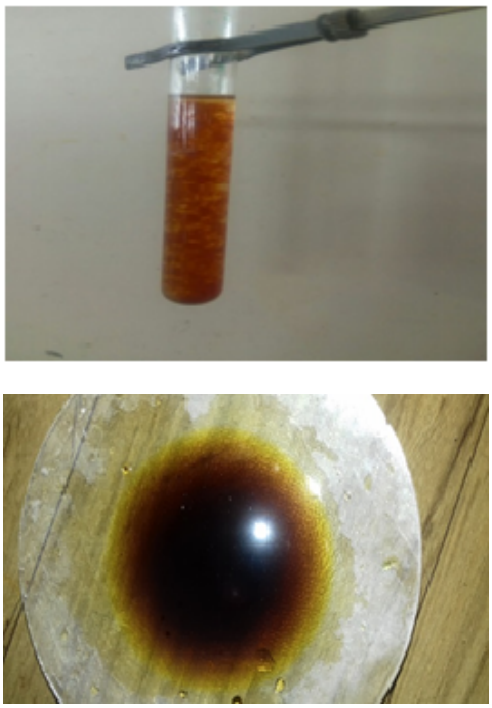

Figure 8. Confirmative test for Al and Mg elements.

Table 1. Qualitative analysis of Mg and Al.

Test	Observation	Inference
Test for Mg^{+2}		
CS + Magneson solution + NaOH	Red ppt obtained	Mg^{+2} present and confirmed
Test for Al^{+3}		
CS + NaOH on a plate + Alizarin red acetic acid till violet just disappear	Red colouration	Al^{+3} present and confirmed

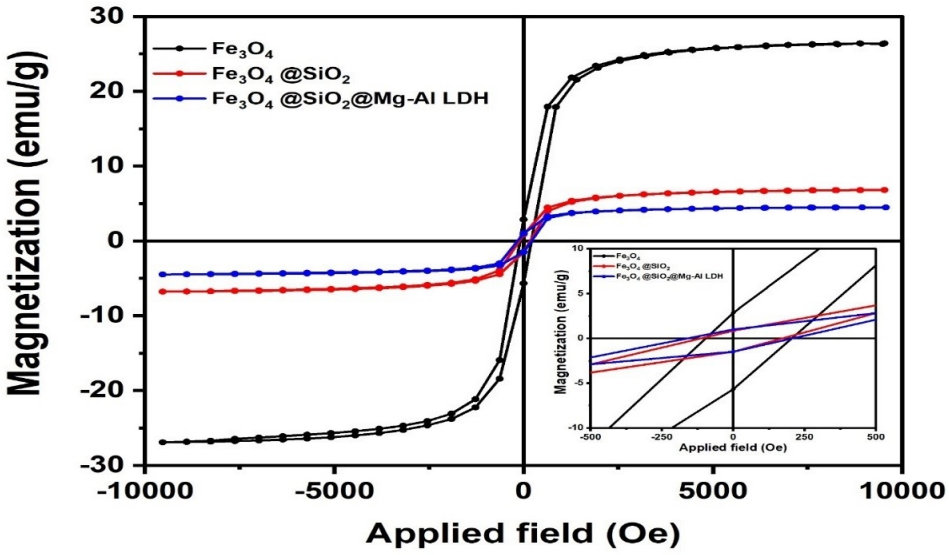

Figure 9. VSM of: Fe_3O_4 (a), Fe_3O_4@SiO_2 (b) and Fe_3O_4@SiO_2@Mg-Al LDH (c).

for excellent product isolation (entry 3, Table 4).

Further to check reaction rate with other techniques available in the author laboratory, including room temperature stirring, ultrasonic irradiation, mechanical and microwave irradiation performed set of reaction in a model optimized reaction condition for the synthesis of 2-amino-4H-chromene derivatives (Table 5). Based on our optimization study, stirring, ultrasonication, and mechanochemistry resulted in less product isolation, and long reaction times (entries 1-3, Table 5). On the other hand, MWI method gave high product isolation in a shorter reaction time (entry 4, Table 5).

To check compatibility of this method for various substituent present on aryl aldehyde examined for chromene derivative synthesis. The aryl aldehyde containing electron withdrawing groups **(EWG)** or electron donating groups **(EDG)** not showed accountable changes in the reaction

Table 2. Data of Ms, Mr, Hc and χ.

Sample	Ms (emu/g)	Mr (emu/g)	Hc (Oe)	χ (emu/g.Oe)
Fe_3O_4	36.11	5.79	347.03	0.00415
Fe_3O_4@SiO_2	28.63	3.53	355.60	0.00234
Fe_3O_4@SiO_2@Mg-Al-LDH	12.65	1.23	360.53	0.000187

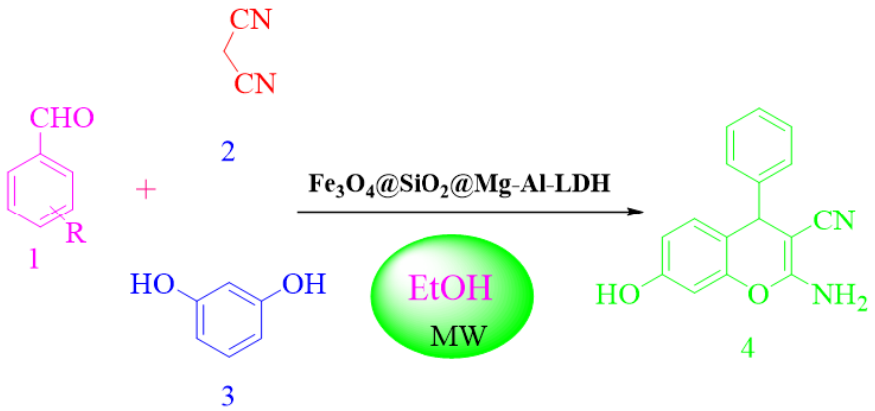

Scheme 1. General reaction of 2-amino-4H-chromene synthesis .

Table 3. Optimization of reaction conditions.

Entry	Catalyst (mg)	Time (min)	Yield[a]
1	0	5	Nil
2	5	5	Nil
2	10	5	30
3	20	**5**	40
4	**25**	5	**90**
5	30	5	90
6	35	5	90

* 1 mmol of each Aryl aldehyde, malononitrile, and resorcinol, in ethanol, MW@300W.
[a] The conversion was monitored by TLC, and isolated product represented in % of yield.

Table 4. Microwave power optimization rate of the reaction.

Entry	Methods	Power (W)	Time (min)	Yield (%)
1	MWI	100	5	78
2	MWI	180	5	81
3	**MWI**	**300**	**5**	**90**
4	MWI	450	5	90
5	MWI	600	5	90

* 1 mmol of each aryl aldehyde, malononitrile, & resorcinol in ethanol.

time as well as final product isolation (Table 6). Hence, the present developed method and catalysts is compatible with wide range of aryl aldehyde substituents gave high product yield, faster reaction rate and reusable catalysts.

3.3 A possible route for the product formation

Scheme 2 shows the probable mechanism of the synthesis of 2-amino-4H-chromene derivatives catalyzed by Fe_3O_4@SiO_2-Mg-Al-LDH. The reaction is initially preceded by the Knoevenagel condensation reaction between aryl aldehyde **(1)** and ethyl cyanoacetate or malononitrile **(2)**. In the subsequent step, the Knoevenagel adduct formed in the previous step reacted with resorcinol **(3)** to lead to an intermediate compound followed by aromatization and then intramolecular cyclization in the existence of WEOFPA which gave us of the 2-amino-4H-chromene product **(5)**.

3.4 Biological activity

Furthermore evaluated antimicrobial activities of some of the selected 2-amino-4H-chromene derivatives (**4b**, **4c** & **4d**) employing the disk method by clinical and laboratory standards institute [57]. The antimicrobial inhibition assay was carried out *in vitro* agar media at incubation of 37 °C. The compounds **4b**, **4c**, and **4d** showed comparable activity tested against bacteria and fungi. The derivatives **4c** and **4d** showed activity of *Bacillus*, and other derivatives **4b**, **4c** and **4d** showed average activity against *Candida*. But

Table 5. Various optimized techniques in a model reaction.

Entry	Methods	Time (min)	Yield (%)
1	rt	70	61
2	Ultrasonication	80	55
3	Mechanical	35	30
4	**MWI**	**5**	**90**

compound **4b** inhibited against *A. niger* while other compounds showed less activity. The detailed evaluation of the antibacterial and antifungal activities of the compounds tested is tabulated in Table 7.

The Structure Activity Relationship (SAR) between molecular structure and its biological activity is discussed based on the above outcomes. Several key factors of structural aspects of the derivatives (**4b**, **4c**, and **4d**) are considered. The biological effects of a chemical compound can often be predicted from its molecular structure due to similar or isosteres compounds having similar physical and biological properties. From the obtained *in vitro* results of antimicrobial activities, 2-amino-4H-chromene derivatives **4b** showed less activity compared to derivatives **4c** & **4d** for *E. coli*. This is due to the presence of structural difference in aryl aldehyde, where **4c** & **4d** contain pyridine ring systems, and such type of environment is not present in **4b**. Similar trends were also noticed for *Bacillus subtilis* and *Pseudomonas* strains. However, in the case of *Candida*, more sensitive activity trends were noticed compared to the above two types of microbes. In the case of *A. niger*, compound **4b** showed better activity compared to the other two derivatives, **4c** and **4d**, due to the presence of hydroxy and bromo groups in the benzene ring and not containing such kind of substituent environment in the other two derivatives.

3.5 Reusability of the catalysts

To check prepared heterogeneous catalysts reusability properties examined in a model reaction under optimized above reaction condition, and catalysts quantity. After the reaction completion monitored by TLC, the catalysts separated from the reaction, adding ethanol followed by filtration, and washed catalysts with a sequence of water, and ethanol, and dried on an oven 2 h at about 80 °C. Then, the catalyst was reused for the next cycle in a model reaction and followed the procedure of the first cycle. Up to five cycles of reaction performed on a model reaction using same catalysts reused and isolated yields 93, 90, 89, 87 and 80% for first to fifth cycles, respectively. In case of fifth cycle of reused catalysed reaction gave 13% loss in the final product isolation across the 5 cycles, this revealed up to fourth cycle catalysts can be reused without noticeable product isolation (Fig. 10). The recycled catalyst morphology and composition examined using XRD, FT-IR, FE-SEM and EDS (Fig. S21, S22, S24 & S25). These data revealed that, slight change in the morphology and diffraction pattern of the catalysts, but element composition intact. An external magnet helping easy separation of the catalyst in this study, since it is heteroge-

Table 6. Structure and physical constant of 2-amino-4H-chromene derivatives.

Entry	Benzaldehyde	Product	Reaction time (min)	Yield[b] (%)	m.p (°C)	
					Obs.	Rep.
1	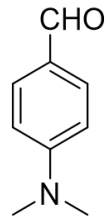	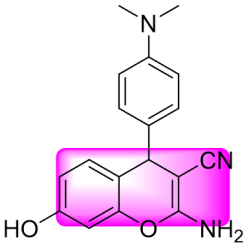 **4a**	5	89	233-235	New
2	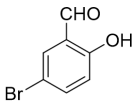	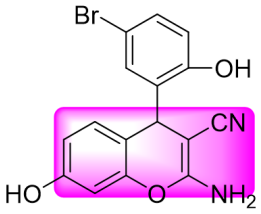 **4b**	5	95	280-282	New
3	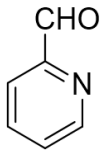	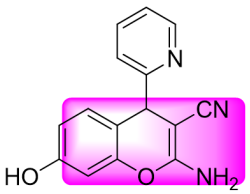 **4c**	5	96	290-292	New
4	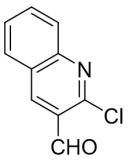	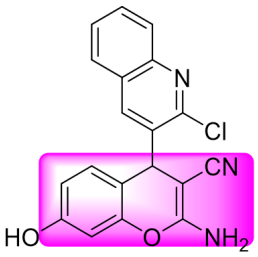 **4d**	5	94	285-286	New
5	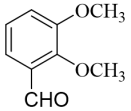	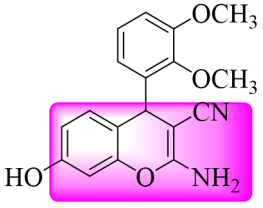 **4e**	5	90	184-186	185-187 [49]

Table 6. Continued of Table 6.

Entry	Benzaldehyde	Product	Reaction time (min)	Yield[b] (%)	m.p (°C)	
					Obs.	Rep.
6	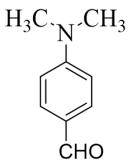	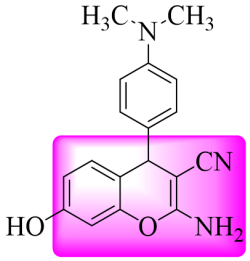 **4g**	5	91	206-207	205-206 [50]
7	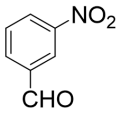	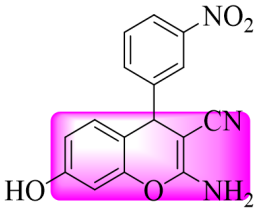 **4h**	5	91	171-172	170-171 [51]
8	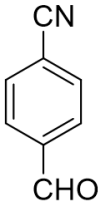	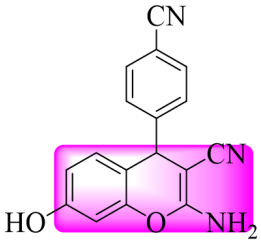 **4i**	5	88	179-181	180-182 [52]
9	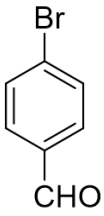	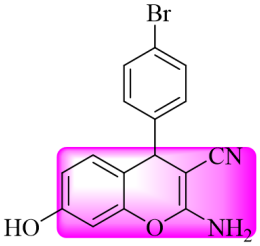 **4j**	5	87	186-188	185-187 [53]
10	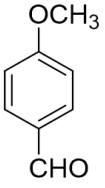	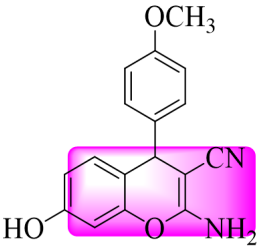 **4k**	5	90	110-112	112-113 [54]

Table 6. Continued of Table 6.

Entry	Benzaldehyde	Product	Reaction time (min)	Yield[b] (%)	m.p (°C)	
					Obs.	Rep.
11	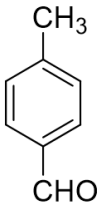	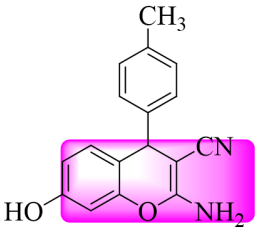 **4l**	5	91	183-185	184-186 [55]
12	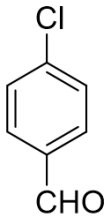	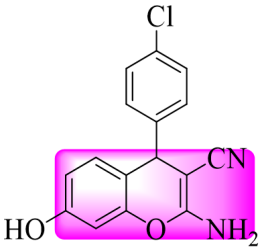 **4m**	5	89	160-161	162-163 [56]

neous and hold catalysts externally and separate catalysts. In addition, with only a small quantity of material required for the reaction and the ability to reuse it for four cycles, gave minimal waste production.

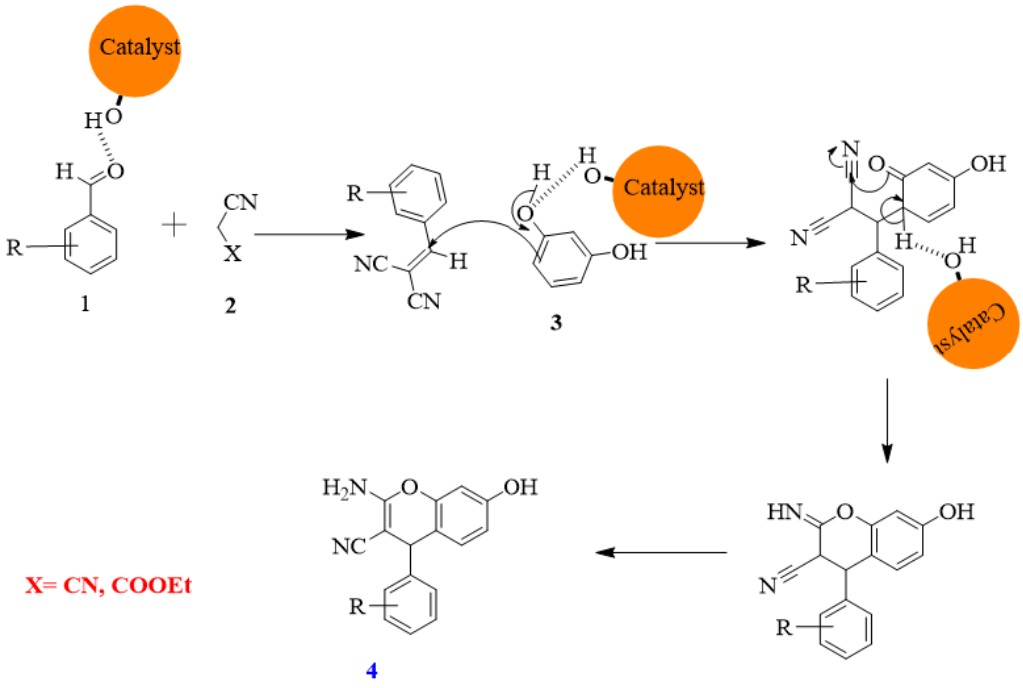

Scheme 2. Mechanism of Formation of 2-amino-4H-chromene derivative.

Table 7. Antimicrobial activity of 2-amino-4H-chromene derivatives.

	Organisms	Compounds	75 μl/mL	50 μl/mL	25 μl/mL	10 μl/mL	5 μl/mL
Antibacterial activity	*E. coli*	**4b**	20 mm	R	R	R	R
		4c	15 mm	15 mm	R	R	R
		4d	15 mm	15 mm	R	R	R
	Ciprofloxacin		-	-	-	-	**30 mm**
	Bacillus subtilis	**4b**	23 mm	R	R	R	R
		4c	25 mm	20 mm	R	R	R
		4d	17 mm	23 mm	R	R	R
	Ciprofloxacn		-	-	-	**32 mm**	**35 mm**
	Pseudomonas	**4b**	17 mm	R	R	R	R
		4c	23 mm	20 mm	R	R	R
		4d	15 mm	15 mm	R	R	R
	Ciprofloxacin		-	-	**45 mm**	-	-
Antifungal activity	*Candida*	4b	17 mm	15 mm	R	R	R
		4c	25 mm	20 mm	15 mm	R	R
		4d	23 mm	20 mm	18 mm	R	R
	Fluconazole		-	-	**35 mm**	-	-
	A. niger	**4b**	15 mm	20 mm	15 mm	R	R
		4c	18 mm	17 mm	R	R	R
		4d	20 mm	23 mm	R	R	R
	Fluconazole		-	-	**28 mm**	-	-

The catalytic efficiency of the present method for the 2-amino-4H-chromene derivatives synthesis was compared with the previously reported methods (Table 8). In Table 8, some of the catalysts previously reported are expensive, use of hazardous organic solvent, high temperature, excess reagent and long reaction time (entries 1, 4 & 6, Table 8). Hence, the present developed method showed added advantages like faster reaction rate, inexpensive, high yield, eco-friendly, and not required chromatographic purification compared to other reported methods.

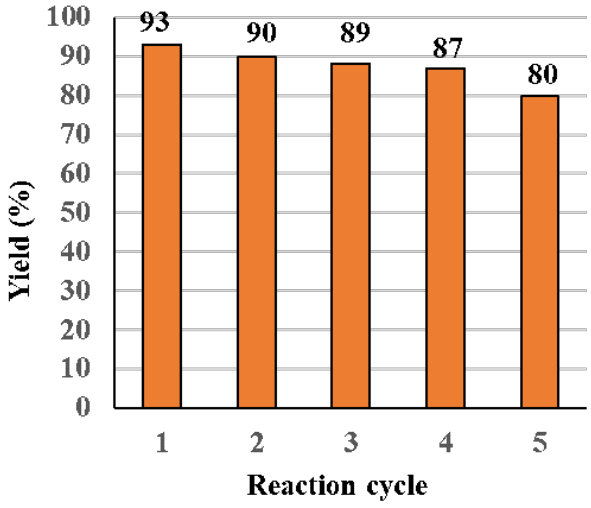

Figure 10. Reusability of the catalysts.

4. Conclusion

The present study demonstrates required MNPs core shell is prepared by agro-waste extract medium, and then functionalized further to achieve better stability and activity. The application of the prepared heterogeneous catalysts described for the synthesis of 2-amino-4H-chromene derivatives via MCRs of aryl/heterocyclic aldehydes (1), malononitrile (2) and resorcinol (3). The developed method showed several advantages such as non-toxic, eco-friendly, recycle and being affordable, simple, and recyclable. Moreover, it is simple to separate isolated products from

Table 8. Comparison of reported with present method.

Entry	Catalyst	Condition	Time (min)	Yield (%)	[Ref.]
1	Fe_3O_4	Ethylene glycol	60	93	[58]
2	MNP@AVOPc	rt/Solvent free	116	94	[59]
3	Nano Al_2O_3	rt/EtOH	280	89	[60]
4	α-Fe_2O_3	80 °C/H_2O	40	89	[61]
5	$Mg(ClO_4)_2$	Ethanol solvent free	60	80	[62]
6	KF/Al_2O_3	rt/DMF	120-140	81	[63]
7	MNPs@Cu	90 °C/Solvent free	10	95	[64]
8	Pbo NPs	Neat, grinding	20	91	[65]
9	APTES@Fe_3O_4	Water	90	92	[66]
10	Nanocrystalline MgO	Rt	180	62	[67]
11	MNPs-Fe_3O_4/PCL	80 °C/EtOAc free	45	94	[68]
12	ZnO NPs	Reflux/EtOH	10	80	[69]
13	**Fe_3O_4@SiO_2@Mg-Al-LDH**	**MWI/EtOH**	**5**	**95**	**[present work]**

catalysts by filtration, and recrystallization in ethanol provides pure derivatives without requirement of column chromatographic purification. The obtained products were analysed through FT-IR, LC-MS, ^{1}H & ^{13}C-NMR spectroscopy. Further, the selected derivatives tested for their biological activities and showed comparable activity with reference used.

Acknowledgement
The authors are thankful to the SERB-SURE, GOI (SUR/2022/002631) and RCUB (RCU-IDR-2022-23) for the financial support to Dr. KK.

Authors contributions
Authors have contributed equally in preparing and writing the manuscript.

Availability of data and materials
The data that support the findings of this study are available from the corresponding author upon reasonable request. FT-IR, ^{1}H-NMR, and LC-MS of the selected compounds are available in supplementary.

Conflict of interests
The authors declare that they have no known competing financial interests or personal relationships that could have appeared to influence the work reported in this paper.

References

[1] V. Y. Sosnovskikh, V. Y. Korotaev, D. L. Chizhov, I. B. Kutyashev, D. S. Yachevskii, O. N. Kazheva, O. A. Dyachenko, and V. N. Charushin. , *J. Org. Chem.*, **12**(2006):4538–43.
DOI: https://doi.org/10.1002/ejoc.201500737.

[2] M. Terada and K. Sorimachi. *J. Chem. Soc.*, **129**(2007):292–3.
DOI: https://doi.org/10.1016/j.bbamem.2013.07.011.

[3] T. Ogoshi, S. Kanai, S. Fujinami, T.-A. Yamagishi, and Y. Nakamoto. *J. Am. Chem. Soc.*, **15**(2008):5022–3.
DOI: https://doi.org/10.1021/jo100273n.

[4] N. M. Sabry, H. M. Mohamed, E. S. A. E. H. Khattab, S. S. Motlaq, and A. M. El-Agrody. *Eur. J. Med. Chem.*, **2**(2011):765–72, .
DOI: https://doi.org/10.5155/eurjchem.5.1.133-137.923.

[5] S. R. Kolla and Y. R. Lee. *Tetrahedron.*, **68**(2012):226–37, .
DOI: https://doi.org/10.1080/00397911.2018.1468467.

[6] A. Khalafi-Nezhad, S. Sarikhani, E. S. Shahidzadeh, and F. Panahi. *Green Chem.*, **10**(2012):2876–84, .
DOI: https://doi.org/10.1039/C2GC35765H.

[7] H. Adibi, R. Khodarahmi, K. Mansouri, M. Khaleghi, and S. Maghsoudi. *J. Fac. Pharm.*, **19**(2013):23–30, .
DOI: https://doi.org/10.13005/ojc/320453.

[8] P. P. Ghosh and A. R. Das. *J. Org. Chem.*, **12**(2013):6170–81, .
DOI: https://doi.org/10.1016/j.rechem.2023.101215.

[9] R. Mohammadi and M. Z. Kassaee. *J. Mol. Catalysis.*, **380**(2013):152–8, .
DOI: https://doi.org/10.1016/j.molcata.2013.09.027.

[10] G. H. Li, Z. Fang, and S. Yang. *ACS Sust. Chem. Eng.*, **4**(2016):236–246.
DOI: https://doi.org/10.1021/acssuschemeng.5b01480.

[11] J. A. Wang, P. Sudarsanam, Y. Xu, H. Zhang, H. Li, and S. Yang. *Green Chem.*, **22**(2020):2997–3012. DOI: https://doi.org/10.1039/D0GC00924E.

[12] F. Poovan, V. G. Chandrasekhar, K. Natte, and R. V. Jagadeesh. *Catal. Sci. Technol.*, **12**(2022):6623–6649. DOI: https://doi.org/10.1039/D2CY00232A.

[13] C. M. Hendrich, K. Sekine, T. Koshikawa, K. Tanaka, A. Stephen, and K. Hashmi. *Chem. Rev.*, **14**(2021):9113–9163. DOI: https://doi.org/10.1021/acs.chemrev.0c00824.

[14] N. M. Sabry, H. M. Mohamed, E. S. A. E. H. Khattab, S. S. Motlaq, and A. M. El-Agrody. *Eur. J. Med. Chem.*, **2**(2011):765–72, . DOI: https://doi.org/10.1016/j.ejmech.2010.12.015.

[15] S. R. Kolla and Y. R. Lee. *Tetrahedron*, **1**(2012):226–37, . DOI: https://doi.org/10.1016/j.tet.2010.09.050.

[16] A. Khalafi-Nezhad, S. Sarikhani, E. S. Shahidzadeh, and F. Panahi. *Green Chem.*, **10**(2012):2876–84, . DOI: https://doi.org/10.1039/c2gc35765h.

[17] H. Adibi, R. Khodarahmi, K. Mansouri, M. Khaleghi, and S. Maghsoudi. *J. Fac. Pharm.*, **19**(2013):23–30, . DOI: https://doi.org/10.1002/jccs.201900554.

[18] P. P. Ghosh and A. R. Das. *J. Org. Chem.*, **12**(2013):6170–81, . DOI: https://doi.org/10.1021/jo400763z.

[19] R. Mohammadi and M. Z. Kassaee. *J. Mol. Catal. A. Chem.*, **380**(2013):152–8, . DOI: https://doi.org/10.1016/j.molcata.2013.09.027.

[20] G. Brahmachari and S. Laskar. *Polycycl. Aromat. Compd.*, **8**(2014): 873–88. DOI: https://doi.org/10.1515/9783110985313-001.

[21] M. A. Ghasemzadeh, M. H. Abdollahi-Basir, and M. Babaei. *Green Chem. Lett. Rev.*, **4**(2015):40–9. DOI: https://doi.org/10.1080/17518253.2015.1107139.

[22] A. Maleki, R. Ghalavand, and R. Firouzi Haji. *Appl. Organomet. Chem.*, (2018):e–3916. DOI: https://doi.org/10.1002/aoc.3916.

[23] D. Elhamifar, Z. Ramazani, M. Norouzi, and R. Mirbagheri. *J. Colloid Interface Sci.*, **511**(2018):392–401. DOI: https://doi.org/10.1016/j.jcis.2017.10.013.

[24] A. Maleki and S. Azadegan. *Inorg. Nano-Met. Chem.*, **6**(2017):917–24, . DOI: https://doi.org/10.1080/24701556.2019.1577258.

[25] A. Maleki and S. Azadegan. *J. Inorg. Organomet. Polym. Mater.*, **3**(2017):714–9, . DOI: https://doi.org/10.1007/s10904-017-0514-z.

[26] A. Maleki. *Ultrason. Sonochem.*, **40**(2018):460–4, . DOI: https://doi.org/10.1016/j.ultsonch.2017.07.020.

[27] A. H. Lu, E. L. Salabas, and F. Schuth. *Angew. Chem., Int. Ed. Engl.*, **8**(2007):1222–44, . DOI: https://doi.org/10.1002/anie.200602866.

[28] A. H. Lu, W. Schmidt, N. Matoussevitch, H. Bonnemann, B. Spliethoff, B. Tesche, E. Bill, W. Kiefer, and F. Schuth. *Angew. Chem., Int. Ed. Engl.*, **33**(2004):4303–6, . DOI: https://doi.org/10.1002/anie.200454222.

[29] S. C. Tsang, I. Paraskevas V. Caps, D. Chadwick, and D. Thompsett. *Angew. Chem., Int. Ed. Engl.*, **40**(2004):5763–7. DOI: https://doi.org/10.1002/anie.200460552.

[30] B. Malekia, H. Natheghia, R. Tayebeea, H. Alinezhadb, A. Amiria, S. A. Hossienic, and S. M. M. Nouri. *Polycycl. Aromat. Compd.*, **40**(2020):633–643. DOI: https://doi.org/10.1080/10406638.2018.1469519.

[31] A. M. Razieh Firouzi-Haji. *Chemistry Select*, **4**(2019):853–857. DOI: https://doi.org/10.1002/slct.201802608.

[32] A. Maleki and R. Firouzi-Haji. *Sci. Rep.*, **8**(2018):17303. DOI: https://doi.org/10.1038/s41598-018-35676-x.

[33] A. Maleki. *RSC Adv.*, **109**(2014):64169–73, . DOI: https://doi.org/10.1039/C4RA10856F.

[34] A. Maleki. *Tetrahedron.*, **38**(2012):7827–33, . DOI: https://doi.org/10.1016/j.tet.2012.07.034.

[35] A. Maleki. *Tetrahedron.*, **16**(2013):2055–9, . DOI: https://doi.org/10.1016/j.tetlet.2013.01.123.

[36] F. Dumitrache, I. Morjan, R. Alexandrescu, R. E. Morjan, I. Voicu, I. Sandu, I. Soare, M. Ploscaru, C. Fleaca, and V. Ciupina. *Diam. Relat. Mater.*, **2**(2004):362–70. DOI: https://doi.org/10.1016/j.diamond.2003.10.022.

[37] J. Zheng, Z. Q. Liu, X. S. Zhao, M. Liu, X. Liu, and W. Chu. *Nat. Nanotechnol.*, **16**(2012):165601. DOI: https://doi.org/10.1088/0957-4484/23/16/165601.

[38] M. Tazari and H. Kiyani. *Curr Org Synth.*, **16**(2019):793–800. DOI: https://doi.org/10.2174/1570179416666190415105818.

[39] A. M. Delfani, K. Hamzeh, and Z. Mehdi. *Bentham Science Publishers*, **17**(2023):1542–1552. DOI: https://doi.org/10.2174/0113852728269951231009060535.

[40] M. Z. Kassaee, H. Masrouri, and F. Movahedi. *RSC Adv.*, **10**(2020): 44946–1, . DOI: https://doi.org/10.1039/d0ra09087e.

[41] M. Z. Kassaee, H. Masrouri, and H. Masrouri. *Appl. Catal.*, **395**(2011):28–33, . DOI: https://doi.org/10.1016/j.apcata.2011.01.018.

[42] M. M. Khafagy, H. F. A. El-Wahas, F. A. Eid, and A. M. El-Agrody. *Farmaco.*, **57**(2002):715–722. DOI: https://doi.org/10.1016/S0014-827X(02)01263-6.

[43] K. Hiramoto, A. Nasuhara, K. Michikoshi, K. Kato, and K. Kikugawa. *Mutat. Res.*, **395**(1997):47–56. DOI: https://doi.org/10.1016/S1383-5718(97)00141-1.

[44] A. G. Martinez and L. J. Marco. *Bio.org Med. Chem. Lett.*, **7**(1997): 3165–3170. DOI: https://doi.org/10.1016/S0960.

[45] S. J. Mohr, M. A. Chirigos, F. S. Fuhrman, and J. W. Pryor. *Cancer Res.*, **35**(1997):3750–3754. DOI: https://doi.org/10.1515/cse-2016-0002.

[46] W. O. Foye. *Principi Di Chemico Farmaceutic Piccin*, **416**(1991).

[47] E. C. Witte, P. Neubert, and A. Roesch. *O.D.E. Ger. Chem. Abstr.*, **104**(1986):2249–15.

[48] F. Y. F. Ren, B. Yang, and X. L. Liao. *Catal. Sci. Technol.*, **6**(2016): 4283–4293. DOI: https://doi.org/10.1039/C5CY01888A.

[49] C. S. Konkoy, D. B. S. X. Fisck, N. C. Cai, J. F. Lan, and W. Keana. *Chem. Abstr.*, **134**(2001):29313a. URL https://www.mdpi.com/2073-4344/11/9/1108.

[50] G. P. Ellis, A. Weissberger, and E. C. Taylor. *Chromeones*, **13**(1977). DOI: https://doi.org/10.37652/juaps.2007.15597.

[51] E. A. A. Hafez, M. H. Elnagdi, A. G. A. Elagamey, and F. M. A. A. El-Taweel. *Heterocycles*, **26**(1987):903–907. DOI: https://doi.org/10.3987/R-1987-04-0903.

[52] Y. He, R. Hu, R. Tong, F. Li, J. Shi, and M. Zhang. *Molecules*, **19**(2014):19253–1. DOI: https://doi.org/10.1002/adma.201705630.

[53] M. A. Wanzheng, M. A. E.G. Abdol, S. S. Mostafa, J. Ramin, and J. Giorgos. *RSC Adv.*, **9**(2019):12801.
DOI: https://doi.org/10.1039/c9ra01679a.

[54] A. Zhu, Q. Li, W. Feng, D. Fan, and L. Li. *Catal. Letters*, **151**(2021): 720–33.
DOI: https://doi.org/10.1007/s10562-020-03332-7.

[55] S. R. Kolla and Y. R. Lee. *Tetrahedron*, **67**(2011):8271–1, .
DOI: https://doi.org/10.1016/j.tet.2011.08.086.

[56] F. O. Chahkamali, S. Sobhani, and J. M. Sansano. *Sci. Rep.*, **12**(2022): 2867.
DOI: https://doi.org/10.1038/s41598-022-06759-7.

[57] P. Singh, P. Yadav, A. Mishra, and S. K. Awasthi. *ACS Omega*, **5**(2020):4223–32.
DOI: https://doi.org/10.1021/acsomega.9b04117.

[58] X. Yu and Z. Zhou. *Phosphorus Sulfur Silicon Relat. Elem.*, (2018): 387–93.
DOI: https://doi.org/10.1080/10426507.2018.1424161.

[59] I. B. Masesane and S. O. Mihigo. *Synth Commun.*, **45**(2015): 1546–51.
DOI: https://doi.org/10.1080/00397911.2015.1031249.

[60] M. G. Dekamin, M. Eslami, and A. Maleki. *Tetrahedron*, **69**(2013): 1074–85.
DOI: https://doi.org/10.1016/j.tet.2012.11.068.

[61] S. Gupta, R. Banu, C. Ameta, R. Ameta, and P. B. Punjabi. *Top. Curr. Chem.*, **13**(2019):377.
DOI: https://doi.org/10.1007/s41061-019-0238-3.

[62] R. L. Magar, P. B. Thorat, V. B. Jadhav, S. U. Tekale, S. A. Dake, B. R. Patil, and R. P. Pawar. *J. Mol. Catal.Chemica.*, **374**(2013): 118–24.
DOI: https://doi.org/10.1016/j.molcata.2013.03.022.

[63] S. K. Kundu and A. Bhaumik. *RSC. Adv.*, **5**(2015):32730–9.
DOI: https://doi.org/10.1039/C5RA00951K.

[64] S. Makarem and A. A. M. Fakhari. *Tetrahedron Lett.*, **49**(2008): 7194–6.
DOI: https://doi.org/10.1016/j.tetlet.2008.10.006.

[65] S. K. Kundu, J. Mondal, and A. Bhaumik. *Dalton Trans.*, **42**(2013): 10515–24.
DOI: https://doi.org/10.1039/C3DT50947H.

[66] R. Eivazzadeh Keihan, S. Bahrami, M. G. Gorab, Z. Sadat, and A. Malek. **12**(2022):10664.
DOI: https://doi.org/10.1038/s41598-022-14844-0.

[67] S. L. Zhenga and L. Chen. *Org. Biomol. Chem.*, **19**(2021):10530.
DOI: https://doi.org/10.1039/d1ob01906f.

[68] R. Heydari, R. Shahraki, M. Hossaini, and A. Mansouri. *Res. Chem. Intermed.*, **43**(2017):4611–4622.
DOI: https://doi.org/10.1007/s11164-017-2900-0.

[69] P. Sharma, M. Gupta, R. Kant, and V. K. Gupta. *RSC Adv.*, **6**(2016): 32052–32059.
DOI: https://doi.org/10.1039/C6RA06523F.